Title

Shear stress regulation of miR-93 and miR-484 maturation through nucleolin

Journal

Proceedings of the National Academy of Sciences of the United States of America, 116(26)

ISSN

0027-8424

Authors

Gongol, Brendan

Marin, Traci

Zhang, Jiao

et al.

Publication Date

2019-06-25

DOI

10.1073/pnas.1902844116

Peer reviewed

Shear stress regulation of miR-93 and miR-484 maturation through nucleolin

Brendan Gongol[a,1], Traci Marin[b,1], Jiao Zhang[a], Shen-Chih Wang[c], Wei Sun[d], Ming He[a], Shanshan Chen[e], Lili Chen[e], Jie Li[e], Jun-Hui Liu[f], Marcy Martin[a], Yue Han[g], Jian Kang[a], David A. Johnson[d], Christian Lytle[d], Yi-Shuan Li[h,i], Po-Hsun Huang[j,k], Shu Chien[a,h,i,2], and John Y.-J. Shyy[a,e,2]

[a]Department of Medicine, University of California, San Diego, CA 92093; [b]Department of Health Sciences, Victor Valley College, Victorville, CA 92395; [c]Department of Anesthesiology, Taipei Veterans General Hospital, 115 Taipei, Taiwan; [d]Division of Biomedical Sciences, University of California, Riverside, CA 92521; [e]Cardiovascular Research Center, School of Basic Medical Sciences, Xi'an Jiaotong University Health Science Center, Key Laboratory of Environment and Genes Related to Diseases, Xi'an Jiaotong University, Ministry of Education of China Xi'an, 710029 Xi'an, China; [f]Department of Clinical Laboratory, First Affiliated Hospital of the Medical School, Xi'an Jiaotong University, 710029 Xi'an, China; [g]Institute of Mechanobiology and Medical Engineering, School of Life Sciences & Biotechnology, Shanghai Jiao Tong University, 200240 Shanghai, China; [h]Department of Bioengineering, University of California, San Diego, La Jolla, CA 92093; and [i]Institute of Engineering in Medicine, University of California, San Diego, La Jolla, CA 92093; [j]Cardiovascular Research Center, National Yang-Ming University, 112 Taipei, Taiwan; and [k]Department of Critical Care Medicine, Taipei Veterans General Hospital, 115 Taipei, Taiwan

Contributed by Shu Chien, May 7, 2019 (sent for review February 22, 2019; reviewed by Hong Chen and Yu Huang)

Pulsatile shear (PS) and oscillatory shear (OS) elicit distinct mechanotransduction signals that maintain endothelial homeostasis or induce endothelial dysfunction, respectively. A subset of microRNAs (miRs) in vascular endothelial cells (ECs) are differentially regulated by PS and OS, but the regulation of the miR processing and its implications in EC biology by shear stress are poorly understood. From a systematic in silico analysis for RNA binding proteins that regulate miR processing, we found that nucleolin (NCL) is a major regulator of miR processing in response to OS and essential for the maturation of miR-93 and miR-484 that target mRNAs encoding Krüppel-like factor 2 (KLF2) and endothelial nitric oxide synthase (eNOS). Additionally, anti–miR-93 and anti–miR-484 restore KLF2 and eNOS expression and NO bioavailability in ECs under OS. Analysis of posttranslational modifications of NCL identified that serine 328 (S328) phosphorylation by AMP-activated protein kinase (AMPK) was a major PS-activated event. AMPK phosphorylation of NCL sequesters it in the nucleus, thereby inhibiting miR-93 and miR-484 processing and their subsequent targeting of KLF2 and eNOS mRNA. Elevated levels of miR-93 and miR-484 were found in sera collected from individuals afflicted with coronary artery disease in two cohorts. These findings provide translational relevance of the AMPK–NCL–miR-93/miR-484 axis in miRNA processing in EC health and coronary artery disease.

shear stress | endothelial cells | miRNA | nucleolin | AMPK

Vascular endothelium responds differentially to pulsatile and oscillatory shear stresses (PS and OS stresses, respectively) which are athero-protective and athero-prone, respectively. Shear stress acting on vascular endothelial cells (ECs) regulates a plethora of microRNAs (miRs), which in turn positively or negatively affect endothelial function. miR maturation is a multistep process involving highly orchestrated events in both the nucleus and cytoplasm. Following transcription in the nucleus, primary miRs (pri-miRs) containing a stem loop structure undergo two sequential cleavage steps initiated by removal of the 3′ and 5′ terminal ends by Drosha, a component of the microprocessor complex. Subsequently, the premiRs are shuttled from the nucleus to the cytoplasm and become truncated, resulting in single-stranded miRs that are 21–23 nucleotides in length. These mature miRs bind to the miR-induced silencing complex (miRISC) containing an argonaute (AGO) protein that targets mRNAs for degradation via miR seed sequence complementarity. In the context of vascular biology, shear stress-regulated miRs modulate EC proliferation, inflammation, nitric oxide (NO) bioavailability, and intercellular communication (1–6). Although the effects of PS and OS on miRs have been well studied, the mechanistic basis for miR processing in ECs responding to distinct shear stress is unknown.

Nucleolin (NCL) is a multidomain protein that shuttles between the nucleus and cytoplasm to coordinate various functions (7). Through four tandem nucleotide-binding domains, NCL binds to RNA stem loop structures containing a UCCCGA consensus sequence (8, 9). With respect to miR processing, NCL can interact with the microprocessor complex in the nucleus to promote the processing of miRs that contain GU-enriched sequences (10). To date, studies of NCL in ECs have focused on proliferation, adhesion, and migration of ECs in angiogenesis associated with tumor biology (11–13). Among the PS-activated kinases, AMP-activated protein kinase (AMPK) regulates cellular homeostasis via phosphorylating targets predominantly containing a βθβXXX(S/T)XXXθ consensus sequence (β = basic amino acid, θ = hydrophobic amino acid, and X = any amino acid) (14, 15). Of relevance here is that the amino acid sequences flanking Ser-328 of NCL (NCL S328) correspond to the consensus sequence for AMPK phosphorylation.

In this study, we identified that NCL S328 is phosphorylated by AMPK and that the phosphorylation state of NCL determines the binding of miR-93 and miR-484 to NCL. In response to PS, AMPK phosphorylates NCL S328, resulting in NCL nuclear localization and subsequent inhibition of the binding of NCL/miR-93 and NCL/miR-484 complexes to the microprocessor complex.

Significance

This work identifies a mechanism by which atheroprone oscillatory shear and atheroprotective pulsatile shear differentially regulate microRNA (miR) biogenesis in the vascular endothelium. Nonphosphorylated nucleolin facilitates the maturation of miR-93 and miR-484, which in turn target Krüpple-like factor 2 and endothelial nitric oxide synthase mRNAs. The translational significance of these findings is provided by the identification of elevated levels of miR-93 and miR-484 in sera from patients with coronary artery disease.

Author contributions: J.Z., S. Chien, and J.Y.-J.S. designed research; B.G., T.M., J.Z., S.-C.W., W.S., M.H., S. Chen, L.C., J.L., J.-H.L., M.M., Y.H., J.K., C.L., and P.-H.H. performed research; B.G. and T.M. analyzed data; and B.G., T.M., D.A.J., Y.-S.L., S. Chien, and J.Y.-J.S. wrote the paper.

Reviewers: H.C., Harvard Medical School; and Y.H., The Chinese University of Hong Kong.

The authors declare no conflict of interest.

[1]B.G. and T.M. contributed equally to this work.

[2]To whom correspondence may be addressed. Email: shuchien@eng.ucsd.edu or jshyy@ucsd.edu.

This article contains supporting information online at www.pnas.org/lookup/suppl/doi:10.1073/pnas.1902844116/-/DCSupplemental.

Published online June 10, 2019.

The inhibition of NCL-dependent miR-93/miR-484 processing promotes EC homeostasis through the elevated expression of Krüppel-like factor 2 (KLF2) and endothelial nitric oxide synthase (eNOS). This AMPK–NCL–miR-93/miR-484 axis introduces an athero-protective mechanotransduction mechanism in ECs.

Results

AMPK Phosphorylation of NCL in ECs in Response to PS. To screen for miR-binding proteins that are likely to participate in miR processing regulated by PS, a four-step in silico screening strategy was used (a flowchart is shown in *SI Appendix*, Fig. S1). Initially, we screened miRbase for miR sequences that are conserved among different mammalian species. Next, the miR sequences that were conserved in human, mouse, and rat were used to screen for miR-binding proteins that contain the consensus RNA-binding sequences defined in the A daTabase of RNA binding proteins and AssoCiated moTifs (ATtRACT) database (https://attract.cnic.es/). Because AMPK regulates atheroprotective flow-sensitive miRs (16, 17), these putative miR-binding proteins were cross-referenced to the AMPK phosphorylation target proteome (14, 15) to identify miR-binding proteins that are also AMPK targets (*SI Appendix*, Fig. S1) (Dataset S1). Finally, the identified miR-binding proteins were annotated with transcriptomic information—for example, RNA-sequencing (RNA-seq) datasets—from PS and OS experiments previously reported (18). A total of 66 miR-binding proteins were thus identified by this four-step screening process (Dataset S2). Among these, NCL was predicted to regulate the largest number of miRs (Fig. 1*A*).

Furthermore, the putative AMPK phosphorylation sites of NCL, namely S328 and S571, were found to be highly conserved among human, mouse, and rat. The location of these two Ser residues at the four-tandem nucleotide binding motifs suggested that their phosphorylation status might alter RNA binding (Fig. 1*B*). Next, we investigated if AMPK could phosphorylate NCL, and if so, whether AMPK phosphorylation of NCL regulated miR processing. In vitro kinase assays demonstrated that phosphate incorporation into NCL occurred only in the presence of AMPK (Fig. 1*C*). Furthermore, treatment of the wild-type ($AMPK^{+/+}$), but not AMPKα1 & AMPKα2$^{-/-}$ ($AMPK^{-/-}$), mouse embryonic fibroblasts (MEFs) with 5-aminoimidazole-4-carboxamide ribonucleotide (AICAR), an AMPK pharmacological activator, shifted the isoelectric point of NCL toward a lower pH (Fig. 1*D*). These results are consistent with AMPK phosphorylation of NCL, because phosphorylated NCL would shift the isoelectric point toward a lower pH. Of the 11-mer NCL peptides containing S328, S571, and the de-phospho Ser-to-Ala mimetics (i.e., S328A and S571A), only the NCL S328 peptide was phosphorylated to a similar extent as the control SAMS peptide (Fig. 1*E*). Additionally, the NCL S328A peptide competitively inhibited SAMS peptide phosphorylation (Fig. 1*F*), indicating the specificity of AMPK phosphorylation of NCL S328. We transfected human umbilical vein endothelial cells (HUVECs) with Flag-tagged NCL (Flag-NCL) wild type or Flag-NCL S328A mutant, and then stimulated the transfected cells with AICAR. Immunoprecipitation (IP) with anti-Flag antibody and immunoblotting with anti–phospho-Ser antibody showed significantly greater NCL S328 phosphorylation compared with cells transfected with NCL S328A constructs (Fig. 1*G*). With a newly created antiphospho-NCL S328, we found that NCL S328 phosphorylation in HUVECs was higher under PS than with OS (Fig. 1*H*). The higher level of phosphorylation of NCL S328 was also evident in the mouse thoracic aorta (TA), which is exposed to atheroprotective flow, in comparison with the aortic arch (AA), which experiences atheroprone flow (Fig. 1*I*). In summary, the results illustrated in Fig. 1 demonstrate that PS increases NCL S328 phosphorylation via AMPK in HUVECs.

NCL Involvement in Flow-Regulated miR. To investigate the functional consequences of NCL S328 phosphorylation, cellular fractionation of HUVECs revealed nuclear localization of NCL upon AMPK activation with AICAR, which had little effect when AMPK was knocked down (Fig. 2*A*). These results were validated in HUVECs treated with AICAR or metformin (an AMPK agonist) and immunostained with anti-NCL (*SI Appendix*, Fig. S2*A*). However, little changes in NCL expression were detected in HUVECs stimulated with AICAR or PS (*SI Appendix*, Fig. S2 *B* and *C*). With respect to miR processing in ECs under different flow patterns, NCL interaction with the miR microprocessor Drosha was higher under OS than with PS (Fig. 2*B*). The OS-increased interaction between NCL and Drosha was mimicked by HUVECs transfected with NCL S328A (dephosphomimetic mutant) compared with NCL S328D (phosphomimetic mutant) (Fig. 2*C*). These results suggested that NCL regulates miR processing in ECs in part due to increased NCL binding to Drosha

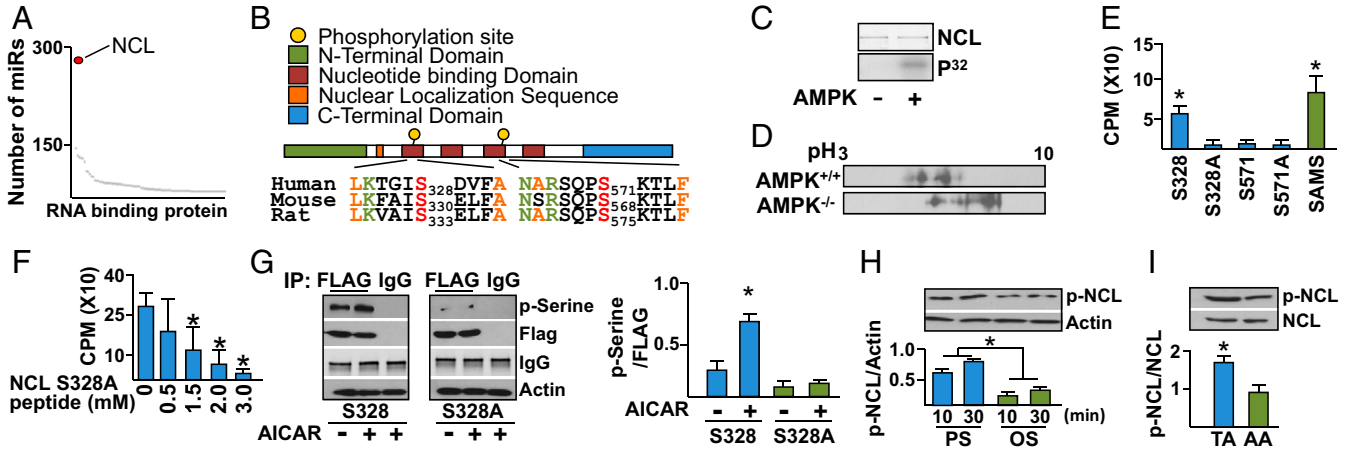

Fig. 1. AMPK phosphorylation of NCL. (*A*) miR binding protein ranking based on the number of putative targeted miRs. (*B*) Functional domains and AMPK phosphorylation consensus sequences on human, mouse, and rat NCL. (*C*) In vitro kinase assay demonstrating the phosphorylation of recombinant NCL by AMPK. (*D*) Isoelectric focusing of NCL isolated from $AMPK^{+/+}$ and $AMPK^{-/-}$ MEF cells. (*E*) In vitro kinase assay using recombinant AMPK and NCL peptides (11-mers) illustrated in *B*. (*F*) Peptide competition assay against SAMS peptide and increasing concentrations of S328A 11-mer peptide. (*G*) Immunoblot with p-Serine antibody for FLAG-NCL immunoprecipitated from HUVEC treated with AICAR for 10 min. (*H* and *I*) Immunoblotting of lysates from HUVECs under PS and OS as well as TA and AA. $^*P < 0.05$. Data are mean ± SEM from three independent experiments.

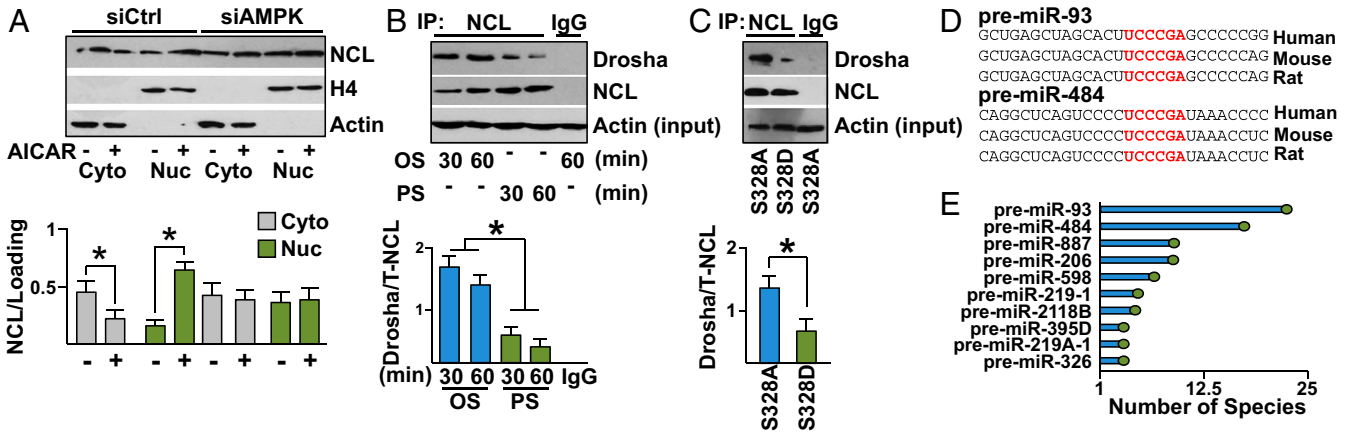

Fig. 2. NCL regulation of miR processing. (*A*) Immunoblot showing the nuclear and cytoplasmic fractionation of NCL in HUVECs treated with or without AICAR, control siRNA (siCtrl), and siAMPK. (*B* and *C*) NCL was immunoprecipitated from HUVECs subjected to OS or PS or transfected with NCL S328A or S328D. Immunoblotting was then performed with anti-Drosha and anti-NCL. (*D*) The NCL binding sequence on miR-93 and miR-484 target sequence for human, mouse, and rat. (*E*) The number of species (i.e., human, mouse, rat, and so forth) that have predicted interaction between NCL and the indicated miRNAs (17 for premiR-93 and 10 for premiR-484). $*P < 0.05$. Data are mean ± SEM from three independent experiments (*A*–*C*).

(19). Furthermore, the premiRs containing UCCCGA required for NCL/RNA binding (20) were ranked based on the conservation of this binding sequence among mammalian species (shown in Dataset S1). Through this screening process, miR-93 (in which both -3p and -5p strands are expressed) and miR-484 were identified to contain the UCCCGA sequence for NCL binding, while exhibiting the highest degree of species conservation including human, mouse, and rat (Fig. 2 *D* and *E* and *SI Appendix*, Table S1).

NCL Regulates Processing of miR-93 and miR-484. Given that PS and OS differentially regulate AMPK activity (21) and that AMPK can phosphorylate NCL (Fig. 1), we investigated the role of AMPK in NCL-regulated miR-93 and miR-484 processing. As illustrated in Fig. 3*A*, the levels of miR-93 and miR-484 were lower in HUVECs exposed to PS compared with OS. This difference in expression level was not observed in cells transfected with AMPK siRNA (siAMPK) (Fig. 3*A*). Similar results were obtained with AMPK$^{-/-}$, compared with AMPK$^{+/+}$ MEFs (*SI Appendix*, Fig. S3*A*). Given that AMPK phosphorylates NCL S328 under PS, HUVECs were transfected with plasmids overexpressing wild-type NCL S328, NCL S328A, or NCL S328D. As illustrated in Fig. 3*B*, the expression levels of miR-93 and miR-484 were higher in HUVECs overexpressing NCL S328A compared with NCL S328 or NCL S328D. Furthermore, NCL binding to premiR-93 and premiR-484 was also increased in cells overexpressing NCL S328A and decreased in HUVECs overexpressing NCL S328D (*SI Appendix*, Fig. S3*B*). Because OS increased the binding of NCL to Drosha (Fig. 2*C*), we investigated whether OS regulates the processing of miR-93 and miR-484, thereby increasing their expression levels. As illustrated in Fig. 3*C*, the binding of premiR-93 and premiR-484 to NCL was attenuated in cells under PS compared with OS. However, such differential binding of premiR-93/484 to NCL was not observed if AMPK was knocked down (Fig. 3*C*). Similar results were observed in experiments with AMPK$^{+/+}$ and AMPK$^{-/-}$ MEFs (*SI Appendix*, Fig. S3*C*) and HUVECs infected with adenovirus overexpressing the constitutively activated AMPK (Ad-AMPK, simulating PS activation of AMPK) (*SI Appendix*, Fig. S3*D*). To confirm the involvement of NCL in OS-mediated premiR-93 or premiR-484 processing, HUVECs were transfected with control or NCL siRNA together with plasmids overexpressing premiR-93 or premiR-484 (simulating OS induction) followed by analyzing the binding of miR to miRISC complex (i.e., AGO2). As illustrated in *SI Appendix*, Fig. S3*E*, miR-93 and miR-484 overexpression resulted in the increased binding of miR-93 and miR-484 to AGO2, which was not seen in HUVECs transfected with NCL siRNA. Moreover, the levels of AGO2-associated miR-93 and miR-484 were higher in

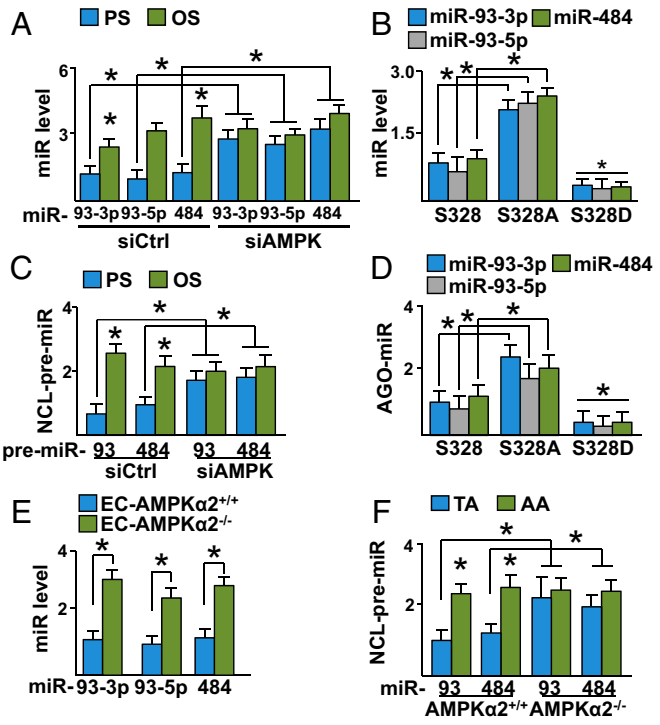

Fig. 3. NCL regulates miR-93 and miR-484 processing. (*A*) Levels of miR-93-3p, miR-93-5p, and miR-484 in HUVECs transfected with control or siAMPK and then subjected to PS or OS for 3 h. (*B*) miR levels in HUVECs transfected with NCL S328, S328A, or S328D. (*C*) NCL was immunoprecipitated from HUVECs transfected with siCtrl or siAMPK and subjected to PS or OS. Levels of premiR-93 and premiR-484 bound to the immunoprecipitated NCL were measured. (*D*) AGO2 was immunoprecipitated from HUVECs transfected with NCL S328, S328A, or S328D. The levels of AGO2-associated miR-93-3p, miR-93-5p, and miR-484 were measured. (*E*) Levels of miR-93-3p, miR-93-5p, and miR-484 in the TA of EC-AMPKα2$^{+/+}$ or EC-AMPKα2$^{-/-}$ mice. (*F*) NCL was immunoprecipitated from the TA or AA from AMPKα2$^{+/+}$ or AMPKα2$^{-/-}$ mice. The NCL-bound miR-93 and miR-484 were then measured. $*P < 0.05$. Data are mean ± SEM from three independent experiments.

HUVECs overexpressing NCL S328A compared with S328 or S328D (Fig. 3*D*). Consistent with these observations, aortic ECs isolated from EC-specific AMPKα2$^{-/-}$ mice (EC-AMPKα2$^{-/-}$) had increased levels of miR-93-3p, miR-93-5p, and miR-484 compared with those from EC-AMPKα2$^{+/+}$ littermates (Fig. 3*E*). Furthermore, the levels of miR-93 and miR-484 and their associations with NCL were higher in the mouse AA than those in TA (Fig. 3*F* and *SI Appendix*, Fig. S3*F*). Taken together, the results summarized in Fig. 3 and *SI Appendix*, Fig. S3 suggest that PS down-regulates, while OS up-regulates, miR-93 and miR-484 processing, which are dependent on AMPK phosphorylation of NCL S328.

NCL Regulation of miR-93 and miR-484 Evokes Endothelial Dysfunction. Because OS promotes endothelial dysfunction (22) and the results illustrated in Fig. 3 showed that OS increases the expression of miR-93 and miR-484, we hypothesized that miR-93 and miR-484 target mRNAs important for EC homeostasis. To identify miR-93 and miR-484 targets, we initially identified mRNAs that are down-regulated in ECs by OS [obtained from our previously generated RNA-seq datasets (18)] and by miR-93 or miR-484 overexpression [obtained from online data mining (23)]. Among the putative mRNA targets (Datasets S3 and S4), markers of functional endothelium including KLF2 and eNOS were down-regulated by OS and miR-93 (6, 24) (Fig. 4*A*). Additionally, eNOS was down-regulated by OS and miR-484 (Fig. 4*B*). We also identified that KLF2 and eNOS mRNAs contain a miR-93 seed sequence while eNOS mRNA also contains a miR-484 seed sequence in their 3′UTR (*SI Appendix*, Fig. S4*A*), suggesting that they would be direct targets of miR-93 or miR-484. To validate these in silico predictions, HUVECs were transfected with premiR-93 or premiR-484. As illustrated in Fig. 4*C*, the expression of endogenous KLF2 and eNOS mRNAs was down-regulated by miR-93, whereas eNOS was down-regulated by miR-484. To confirm these results, HUVECs were transfected with miR-93 or miR-484 overexpression plasmid and then subjected to PS. As illustrated in *SI Appendix*, Fig. S4 *B* and *C*, KLF2 and eNOS mRNA levels were attenuated in miR-overexpressing cells compared with control. Additionally, NCL S328A overexpression (simulating OS) reduced the expressions of KLF2 and eNOS mRNAs in HUVECs, and this effect was blocked with anti–miR-93 or anti–miR-484 (Fig. 4*D*). Furthermore, NCL S328A overexpression in HUVECs followed by PS stimulation reduced KLF2 and eNOS mRNA levels (*SI Appendix*, Fig. S4*D*).

The results illustrated in Fig. 4 *A*–*D* demonstrate that OS (mimicked by miR-93, miR-484, or NCL S328A overexpression) down-regulated KLF2 and eNOS through miR-93 and miR-484 induction. To validate a mechanism involving direct targeting of miR-93 or miR-484, NCL S328A was overexpressed in HUVECs followed by AGO2 IP. As illustrated in Fig. 4*E*, KLF2 and eNOS mRNA levels were elevated in the AGO2 immunoprecipitates and were inhibited by the overexpression of anti–miR-93 or anti–miR-484. Furthermore, KLF2 and eNOS protein expression was enhanced in cells transfected with wild type and treated with AICAR. Moreover, NCL S328D and NCL S328A had opposite effects in regulating the expression of KLF2 and eNOS (Fig. 4*F*). To determine if the down-regulation of KLF2 and eNOS by miR-93 or miR-484 attenuated NO bioavailability, HUVECs were transfected with NCL S328D or NCL S328A with or without anti–miR-93 or anti–miR-484 cotransfection. In comparison with NCL S328D-transfected HUVECs, NO bioavailability was attenuated in NCL S328A-transfected HUVECs. However, this attenuation was blocked by cotransfected anti–miR-93 or anti–miR-484 (Fig. 4*G*). Consistent with these results, the mRNA levels of KLF2 and eNOS were both suppressed in the TA region of EC-AMPKα2$^{-/-}$ mice, compared with that in the TA of EC-AMPKα2$^{+/+}$ littermates (Fig. 4*H*). Taken together, the results summarized in Fig. 4 demonstrate that OS down-regulates KLF2 and eNOS, therefore causing EC dysfunction, in part by increasing miR-93 and miR-484 processing via dephosphorylated NCL.

NCL Regulation of miR-93 and miR-484 Is Involved in Coronary Artery Disease. Given that miR-93 and miR-484 were both OS-induced and collectively down-regulated KLF2 and eNOS transcripts that play key roles in regulating endothelial homeostasis, we compared the serum levels of miR-93 and miR-484 in coronary artery disease (CAD) (n = 52) patients to healthy controls (HC) (n = 45) in a discovery cohort (demographics shown in *SI Appendix*, Table S3). The levels of miR-93-3p, miR-93-5p, and miR-484 were significantly higher in CAD patients compared

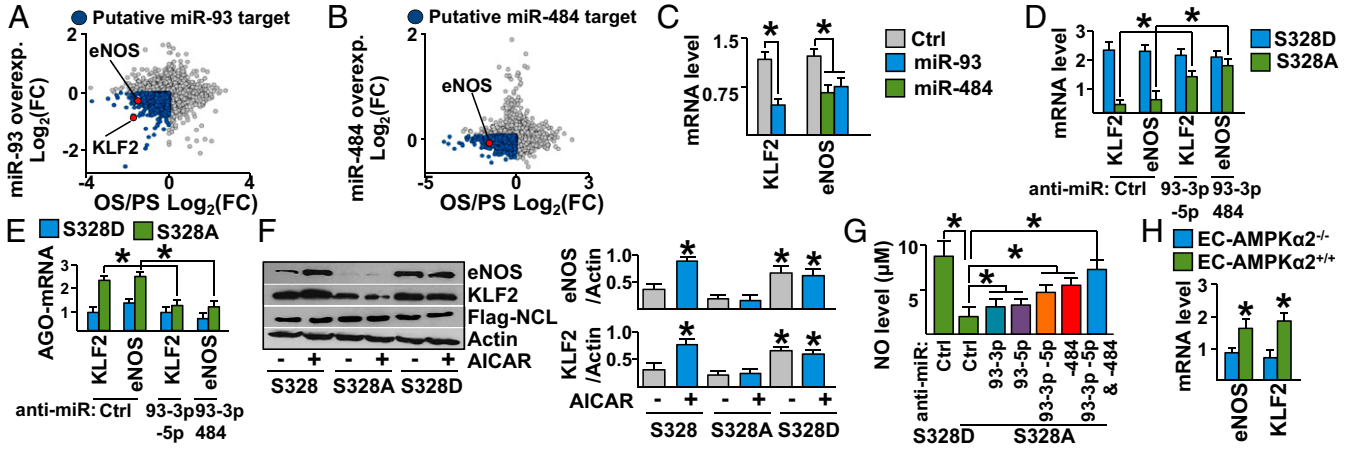

Fig. 4. NCL-miR-93 and NCL-miR4-84 down-regulates KLF2 and eNOS. (*A* and *B*) RNA-seq datasets from OS/PS experiments (18) cross-referenced to those of miR-93 or miR-484 overexpression datasets (GSE86497 and GSE66844). Points in dark blue indicate down-regulated genes in both OS/PS and miR-93 or miR-484 overexpression. Points in blue indicate transcripts down-regulated by miR-93 or miR-484 and OS/PS while points in red indicate eNOS and KLF2. (*C*) KLF2 and eNOS mRNA levels in HUVECs overexpressing premiR-93 or premiR-484. (*D* and *E*) HUVECs were transfected with NCL S328A or S328D in combination with Ctrl siRNA, anti–miR-93, or anti–miR-484. The levels of KLF2 and eNOS mRNA and those bound with AGO2 were measured. (*F*) Immunoblotting of cell lysates from HUVECs transfected with NCL S328, S328A, or S328D and in the presence or absence of AICAR. (*G*) NO bioavailability in HUVECs transfected with NCL S328A or S328D in combination with anti–miR-93 or anti–miR-484. (*H*) KLF2 and eNOS mRNA levels in TA of EC-AMPKα2$^{+/+}$ or EC-AMPKα2$^{-/-}$ mice. *P < 0.05. Data are mean ± SEM from three independent experiments.

with HC individuals (Fig. 5 *A*, *C*, and *E*). Similar results were obtained in the validation cohort containing 32 CAD patients and 31 HC individuals (Fig. 5 *B*, *D*, and *F* and *SI Appendix*, Table S4). Because miR-93 and miR-484 are coregulated by the AMPK–NCL axis (Fig. 3), we examined whether the levels of miR-93-3p, miR-93-5p, and miR-484 were mutually correlated in the sera of CAD patients. As illustrated in Fig. 5*G*, positive correlation was found not only between miR-93-3p and miR-93-5p, but also between miR-93-3p and miR-484 as well as miR-93-5p and miR-484. Collectively, these results suggest that the athero-prone flow-induced miR-93 and miR-484 were elevated in the circulation of most patients diagnosed with CAD in two cohorts.

Discussion

In this investigation, systems studies, including in silico, in vitro, and in vivo experiments, identified shear stress-regulated RNA binding proteins that affect EC biology. The results demonstrate that dephosphorylated NCL under OS facilitates the processing of miR-93 and miR-484, which target KLF2 and eNOS mRNAs to decrease their expression. Moreover, we provide evidence that the PS-activated AMPK regulates miR processing via the phosphorylation of NCL (see Fig. 5*H* for summary). In addition to KLF2 and eNOS, miR-93 and miR-484 were predicted to target many other genes (e.g., bone morphogenetic protein receptor type II) that are also suppressed by OS (Datasets S3 and S4). Thus, NCL-mediated processing of miR-93 and miR-484 represents a mechanotransduction mechanism by which the atheroprone flow down-regulates genes critical for EC homeostasis. Previous studies on mechano-sensitive miRs focused mainly on individual miRNAs, and lack a systems view of their effects on EC function and related diseases (25). Through the identification of a shear stress-regulated miR-binding protein (i.e., NCL) and its regulation at the posttranslational level (i.e., AMPK phosphorylation), our study provides a more comprehensive understanding of the miR networks regulated by shear stress. Moreover, the levels of miR-93 and miR-484 in CAD patient sera, compared with healthy controls, provide a translational implication. The possibility that miR-93 and miR-484 inhibitors have therapeutic benefits deserves further study.

NCL has diverse cellular functions, including transcription, ribosome biogenesis, and angiogenesis, that depend on its cellular localization in response to various stimuli (26). Here, we demonstrate that in response to AMPK activation, phosphorylated NCL is sequestered in the nucleus (Fig. 2 *A*) and impedes premiR-93 and premiR-484 processing by Drosha (Figs. 2 *B* and *C* and 3*C*). The underlying mechanism involves the translocation of phosphorylated NCL from cytoplasm into the nucleus, which inhibits NCL binding Drosha/premiR complexes. In this manner, dephosphorylated NCL would function as a miR nucleus-to-cytoplasm shuttle protein to facilitate the miRISC complex assembly, thus demonstrating AMPK regulation of miR processing. This study focused on the processing of miR-93 and miR-484 by NCL, because of the conservation of the NCL-miR binding sites among mammalian species. Using differentially regulated OS vs. PS miR transcriptomics (27), our bioinformatics analysis identified 17 miRs in addition to miR-93 and miR-484 that are likely to be regulated by AMPK phosphorylation of NCL (*SI Appendix*, Table S2). For example, miR-92a is up-regulated by OS and also predicted to require NCL for processing (*SI Appendix*, Table S2) (6). Additionally, among the miRs containing the NCL binding sequence (Fig. 2*E* and *SI Appendix*, Table S1), miR-219, miR-219-1, and miR-219A-1 are highly homologs to one another. Thus, it is likely that these miRs are orthologs and may require NCL for processing. Thus, OS may regulate, via dephosphorylated NCL, the processing of a network of miRs, which collectively contribute to a transcriptional profile related to dysfunctional endothelium.

In silico prediction of miR/mRNA targeting cannot always be validated experimentally. To enhance the validity of in silico predictions, miR targeting analyses should be correlated not only with the expression level of the target mRNAs (28), but also with changes in cellular functions. In this study, bioinformatics prediction together with biological validation identified that miR-93 and miR-484 target eNOS and KLF2 mRNA. In line with this, anti–miR-93 and anti–miR-484 can rescue NO bioavailability (Fig. 4) (6, 24). Although there are a number of mechanisms that regulate the expression of eNOS, including transcriptional induction by KLF2 (6) and direct phosphorylation (29), miR-93 and miR-484 overexpression was adequate at inhibiting its expression in PS-stimulated ECs. Although a direct interaction between miR-93 and miR-484 was not observed, our findings indicate that they are coregulated by NCL and have similar effects on reducing NO bioavailability. Furthermore, miR-93 and miR-484 are predicted to coregulate a number of targets (Datasets S3 and S4). Collectively, both miR-93 and miR-484 are able to affect eNOS expression directly by targeting eNOS mRNA and indirectly by inhibiting KLF2 induction. Indeed, anti–miR-93 and anti–miR-484 were able to synergistically restore NO bioavailability (Fig. 4*G*).

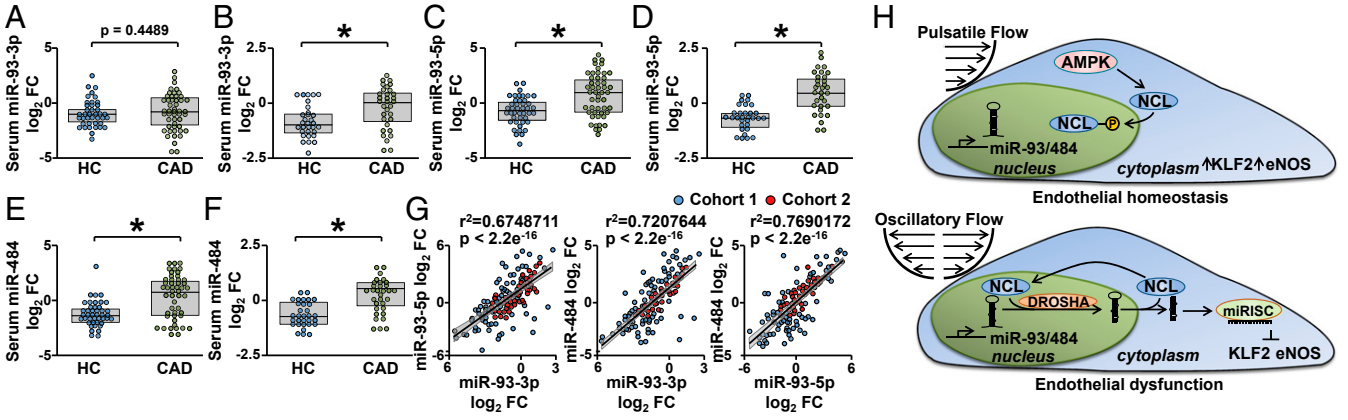

Fig. 5. Higher miR-93 and miR-484 levels in CAD patients. Sera were isolated from patients with CAD ($n = 56$) or HCs ($n = 10$) in the discovery cohort (*A*, *C*, and *E*) and the validation cohort ($n = 32$ and 31, respectively in *B*, *D*, and *F*) and the levels of miR-93-3p, miR-93-5p, and miR-484 were measured. Gray boxes represent the mean and the first and third quantiles; $^*P < 0.05$ (*G*) Correlation among levels of miR-93-3p, miR-93-5p, and miR-484 were found in combined CAD and control samples from both cohorts. (*H*) Graphical abstract of the PS and OS regulation of the NCL-miR93/484 axis via AMPK phosphorylation of NCL, which results in EC homeostasis versus dysfunction.

Although AMPK can directly phosphorylate eNOS, this anti–miR-93/anti–miR-484–mediated restoration is likely due to changes in eNOS protein abundance because the experiment was conducted in the absence of AMPK agonists (29). Consistent with these conclusions are the reports of elevated miR-93 levels found in the vascular wall of subjects with aortic aneurisms (30) and the positive correlation between elevated serum cholesterol and miR-93 levels in human patients (31). However, a negative correlation has been found between miR-93 and ABCA1 levels in macrophages, which impair cholesterol efflux (31). Additionally, elevated miR-484 levels are positively correlated with carcinoma aggressiveness (32). Taken together, we find that miR-93 and miR-484 play a role in endothelial dysfunction and by inference in cardiovascular disease. Indeed, anti–miR-93 and anti–miR-484 had an additive effect to restore NO bioavailability, which is a hallmark of EC homeostasis (6, 24).

In summary, this study provides evidence that the AMPK–NCL axis regulates miR processing. This finding identified a previously unknown role for NCL in endothelial biology in the context of cardiovascular health and disease.

Materials and Methods

Experimental methods are described in detail in *SI Appendix, SI Materials and Methods*. All cells were housed in an incubator filled with 5% CO2 and cultured according to standard protocols. ChIP assays and immunoblotting were conducted according to protocols published by ABcam. A Bio-Rad CFX96 real-time PCR detection system was used with SYBR green (Bio-Rad) for all experiments requiring qPCR analysis. All primers used for ChIP and standard qPCR experiments are displayed in *SI Appendix*, Tables S5 and S6. Bioinformatic analyses were conducted in R programming language with support from Comprehensive R Archive Network (CRAN) and Bioconductor libraries. The human serum studies were approved by the institutional ethics committee of Taipei Veterans General Hospital (discovery cohort) and Xi'an Jiaotong University Medical School (validation cohort).

ACKNOWLEDGMENTS. This work was supported in part by NIH research Grants R01HL106579 and R01HL108735 (to J.Y.-J.S. and S. Chien), Ministry of Science and Technology Academic Excellence Program, Taiwan MOST 107-2633-B-009-003 (to P.-H.H.), and National Natural Science Foundation of China Grant 81500219 (to J.L.).

1. S. Demolli *et al.*, Shear stress-regulated miR-27b controls pericyte recruitment by repressing SEMA6A and SEMA6D. *Cardiovasc. Res.* **113**, 681–691 (2017).
2. Y. Fang, C. Shi, E. Manduchi, M. Civelek, P. F. Davies, MicroRNA-10a regulation of proinflammatory phenotype in athero-susceptible endothelium in vivo and in vitro. *Proc. Natl. Acad. Sci. U.S.A.* **107**, 13450–13455 (2010).
3. X. Qin *et al.*, MicroRNA-19a mediates the suppressive effect of laminar flow on cyclin D1 expression in human umbilical vein endothelial cells. *Proc. Natl. Acad. Sci. U.S.A.* **107**, 3240–3244 (2010).
4. K. C. Wang *et al.*, Role of microRNA-23b in flow-regulation of Rb phosphorylation and endothelial cell growth. *Proc. Natl. Acad. Sci. U.S.A.* **107**, 3234–3239 (2010).
5. M. Weber, M. B. Baker, J. P. Moore, C. D. Searles, MiR-21 is induced in endothelial cells by shear stress and modulates apoptosis and eNOS activity. *Biochem. Biophys. Res. Commun.* **393**, 643–648 (2010).
6. W. Wu *et al.*, Flow-dependent regulation of kruppel-like factor 2 is mediated by microRNA-92a. *Circulation* **124**, 633–641 (2011).
7. C. M. Berger, X. Gaume, P. Bouvet, The roles of nucleolin subcellular localization in cancer. *Biochimie* **113**, 78–85 (2015).
8. V. González, K. Guo, L. Hurley, D. Sun, Identification and characterization of nucleolin as a c-myc G-quadruplex-binding protein. *J. Biol. Chem.* **284**, 23622–23635 (2009).
9. F. Mongelard, P. Bouvet, Nucleolin: A multiFACeTed protein. *Trends Cell Biol.* **17**, 80–86 (2007).
10. F. Pichiorri *et al.*, In vivo NCL targeting affects breast cancer aggressiveness through miRNA regulation. *J. Exp. Med.* **210**, 951–968 (2013).
11. M. Koutsioumpa *et al.*, Interplay between αvβ3 integrin and nucleolin regulates human endothelial and glioma cell migration. *J. Biol. Chem.* **288**, 343–354 (2013).
12. M. Srivastava, H. B. Pollard, Molecular dissection of nucleolin's role in growth and cell proliferation: New insights. *FASEB J.* **13**, 1911–1922 (1999).
13. C. Birmpas, J. P. Briand, J. Courty, P. Katsoris, The pseudopeptide HB-19 binds to cell surface nucleolin and inhibits angiogenesis. *Vasc. Cell* **4**, 21 (2012).
14. B. Gongol, T. Marin, D. A. Johnson, J. Y. Shyy, Bioinformatics approach to identify novel AMPK targets. *Methods Mol. Biol.* **1732**, 99–109 (2018).
15. T. L. Marin *et al.*, Identification of AMP-activated protein kinase targets by a consensus sequence search of the proteome. *BMC Syst. Biol.* **9**, 13 (2015).
16. J. Liu, W. Liu, H. Ying, W. Zhao, H. Zhang, Analysis of microRNA expression profile induced by AICAR in mouse hepatocytes. *Gene* **512**, 364–372 (2013).
17. Y. Zhang *et al.*, AMP-activated protein kinase is involved in endothelial NO synthase activation in response to shear stress. *Arterioscler. Thromb. Vasc. Biol.* **26**, 1281–1287 (2006).
18. N. E. Ajami *et al.*, Systems biology analysis of longitudinal functional response of endothelial cells to shear stress. *Proc. Natl. Acad. Sci. U.S.A.* **114**, 10990–10995 (2017).
19. B. F. Pickering, D. Yu, M. W. Van Dyke, Nucleolin protein interacts with microprocessor complex to affect biogenesis of microRNAs 15a and 16. *J. Biol. Chem.* **286**, 44095–44103 (2011).
20. L. Ghisolfi-Nieto, G. Joseph, F. Puvion-Dutilleul, F. Amalric, P. Bouvet, Nucleolin is a sequence-specific RNA-binding protein: Characterization of targets on pre-ribosomal RNA. *J. Mol. Biol.* **260**, 34–53 (1996).
21. B. Gongol *et al.*, AMPKα2 exerts its anti-inflammatory effects through PARP-1 and Bcl-6. *Proc. Natl. Acad. Sci. U.S.A.* **110**, 3161–3166 (2013).
22. H. Xiao *et al.*, Sterol regulatory element binding protein 2 activation of NLRP3 inflammasome in endothelium mediates hemodynamic-induced atherosclerosis susceptibility. *Circulation* **128**, 632–642 (2013).
23. S. M. Kuosmanen *et al.*, NRF2 regulates endothelial glycolysis and proliferation with miR-93 and mediates the effects of oxidized phospholipids on endothelial activation. *Nucleic Acids Res.* **46**, 1124–1138 (2018).
24. T. P. Shentu *et al.*, AMP-activated protein kinase and sirtuin 1 coregulation of cortactin contributes to endothelial function. *Arterioscler. Thromb. Vasc. Biol.* **36**, 2358–2368 (2016).
25. E. M. Small, E. N. Olson, Pervasive roles of microRNAs in cardiovascular biology. *Nature* **469**, 336–342 (2011).
26. E. Grinstein *et al.*, Cell cycle-controlled interaction of nucleolin with the retinoblastoma protein and cancerous cell transformation. *J. Biol. Chem.* **281**, 22223–22235 (2006).
27. C. J. Holliday, R. F. Ankeny, H. Jo, R. M. Nerem, Discovery of shear- and side-specific mRNAs and miRNAs in human aortic valvular endothelial cells. *Am. J. Physiol. Heart Circ. Physiol.* **301**, H856–H867 (2011).
28. C. Ovando-Vázquez, D. Lepe-Soltero, C. Abreu-Goodger, Improving microRNA target prediction with gene expression profiles. *BMC Genomics* **17**, 364 (2016).
29. V. A. Morrow *et al.*, Direct activation of AMP-activated protein kinase stimulates nitric-oxide synthesis in human aortic endothelial cells. *J. Biol. Chem.* **278**, 31629–31639 (2003).
30. K. Kin *et al.*, Tissue- and plasma-specific MicroRNA signatures for atherosclerotic abdominal aortic aneurysm. *J. Am. Heart Assoc.* **1**, e000745 (2012).
31. Y. He *et al.*, Up-regulated miR-93 contributes to coronary atherosclerosis pathogenesis through targeting ABCA1. *Int. J. Clin. Exp. Med.* **8**, 674–681 (2015).
32. J. Merhautova *et al.*, miR-155 and miR-484 are associated with time to progression in metastatic renal cell carcinoma treated with sunitinib. *BioMed Res. Int.* **2015**, 941980 (2015).